# CORRECTION OF SWITCHING DEAD TIMES IN PWM INVERTER DRIVES

KUN-YONG LEE

FernUniversität/Gesamthochschule
Hagen, Germany

**Abstract.** The paper describes the correction of the switching dead times avoiding a bridge leg short circuit in pulse width modulated voltage sorce inverters. The co consequences on AC variable speed drives with synchronous and asynchronous motors are described by harmonic analysis and by computer simulation.

## INTRODUCTION

Pulsewidth modulated (PWM) voltage source inverters (VSI) for 3-phase load are wide spread feeding standard variable speed or high dynamic controlled asynchronous or synchronous motors. The current control strategies of VSI can be devided into two categories: 1) Tolerance band controllers ("bang-bang" controllers) with variable pulse frequency for direct control of the load currents. 2) PWM controllers with fixed pulse frequency for controlling the load currents through the average load voltage. The effects of the nonideal power switching elements on VSI drives controlled by the second strategy is subject of this paper. Central topic is the switching dead time $T_d$ ("anti overlap time") where both power switches of a bridge leg are turned off avoiding a short circuit of the voltage source during commutation (Fig. 1).
With increasing pulse frequencies the switching dead time takes an increasing part of the pulse period T and thus destores the average load voltage more and more seriously. Basing on this origin there are several consequences on the steady state behaviour of PWM controlled VSI drives:
1) The fundamental amplitudes of load voltages and currents as well as the mean value of motor torque become dependend on the switching dead time and on the operation point - mainly decreasing the magnitudes at motor operation and increasing them at generator operation ([3], [7], [11], [13]).
2) Low order harmonics come up in load voltages and currents and cause a torque ripple with the orders 6n, n=1,2,.. ([7],[10]-[13]).
3) Discontinuous load currents at each zero crossing can occur at low modulation ratios ([7], [11], [13]).
4) Subharmonic oszillations of the entire drive system come up at certain system parameters and operation points ([1]-[6], [13]).
5) All the mentioned effects increase with increasing relative switching dead time $T_d/T$ and with decreasing modulation ratios $a$.
6) If there are superior control loops for current, torque or speed, the mentioned effects are disturbances within these loops and get controlled more or less.

Referring to a 3-phase PWM inverter drive at steady state operation we can take Fig. 1 as a model to define the switching dead time. There are three symmetrical sine wave generators with the fundamental frequency $\omega$, the modulation ratio $a$, the control signals $u_{ca/b/c}$ (reference signals) and a triangle carrier signal with the period time T. In order to avoid a short circuit of the source voltage $U_s$ during commutation the turn ON edges are delayed by the constant turn on delay time $T_{don}$, while the turn OFF edges get directly to the power switches. To define the switching dead time $T_d$, the following simplifications are assumed:
1) The voltage drops of the power switches and of the free wheeling diodes are neglected.
2) The minimum ON/OFF times of the driving or protection circuits are neglected.
3) The additional parasitic turn ON/OFF delay times $T'_{don}$ and $T'_{doff}$ are constant.
4) The commutation occurs apruptly.
According to [7] the switching dead time $T_d$ is defined as the time while both power switches are turned OFF and conduct no current (Eq. 1). In this paper the referred value $\tau_d$ is also called switching dead time.

$$T_d = T_{don} + T'_{don} - T'_{doff} \qquad (1a)$$

$$\tau_d = T_d/T \qquad (1b)$$

## ANALYSIS FOR CONTINUOUS LOAD CURRENTS

Considering the steady state behaviour of the PWM inverter at symmetrical load we can regard only one of the three machine phases since the others operate equal with the exeption of a +/-120° phase shift. In this chapter the effects of the pulse frequency on motor currents and torque (harmonics) are not considered. The remaining fundamental and lower harmonics are considered in the so called "average" values.
During $T_d$ the load current of a bridge leg finds a way through one of the two free wheeling diodes and so its polarity decides whether a small voltage pulse of $U_s T_d$ is added or subtracted from the referred ideal average output voltage $\bar{u}_a(t)$ (Eq. 2a) [7]. With the transformation from the inverter output to the machine phases (Eq. 2b) we get the average load voltage $u_{La}(t)$, normalized on its maximum fundamental amplitude $0.5U_s$ (Eq. 2c). Assuming symmetrical load impedance and defining the time origin with Eq. 2d, we get the ideal part and the voltage change $\Delta u_{La}(t)$ of the average load voltage $u_{La}(t)$ according to Eq. 2e by a harmonic analysis. The angle $\varphi$ is the electrical angle between load voltage and load current. Fig. 2 shows the average voltage change $\Delta u_{La}(t)$.

Fundamentals

Adding the time vectors of the ideal part and of the fundamental voltage change (Fig. 3) we get the fundamental load voltage $u_{La1}(t)$ according to Eq. 3a,b with the angle $\beta$ between the ideal and the changed load voltage (Eq. 3c). Its amplitude is shown in Fig. 4. In steady state operation current, torque and speed of synchronous and asynchronous machines react in the well known ways on the changed fundamental amplitudes of their stator voltage at constant stator frequency.

The fundamental amplitude stays constant for angles $\varphi=\varphi_0$ (Eq. 4a, Fig. 5). To the direction of generator (motor) operation the fundamental amplitude gets increased (decreased) (Eq. 4b, Fig. 6).

If the modulation ratio $a$ is smaller than the fundamental amplitude of the voltage change $8\tau_d/\pi$, the complex time vectors of the voltage fundamentals exist only for angles $\varphi$ greater than a minimum $\varphi_{min}$ (Eq. 5). The minimum $\varphi_{min}$ occurs at $\beta=90°$ (Fig. 7). The angles $\varphi<\varphi_{min}$ can of course occure in real operation and indicate the occurance of discontinuous load currents at each zero crossing (Fig. 8), because in that cases an additional voltage change depending on the "load counter voltage" is added to the load voltage, so the time vector diagram allows angles $\varphi<\varphi_{min}$.

$$\frac{u_{La1}(t)}{0.5\,U_s} = a\,\frac{\sin(\varphi-\beta)}{\sin\varphi}\,\sin(\omega t+\beta) \quad \text{for } \varphi\neq 0$$

$$\frac{\bar{u}_a(t)}{U_s} = 0.5\left(1+\frac{u_{ca}(t)}{U_{cmax}}\right) - \tau_d\,\mathrm{sgn}[i_a(t)] \qquad (2a)$$

$$u_{La}(t) = 2/3\;u_a(t) - 1/3\;[u_b(t)+u_c(t)] \qquad (2b)$$

$$\frac{\bar{u}_{La}(t)}{0.5\,U_s} = \frac{u_{ca}(t)}{U_{cmax}} - \frac{2}{3}\tau_d(2\,\mathrm{sgn}i_a-\mathrm{sgn}i_b-\mathrm{sgn}i_c) \qquad (2c)$$

$$\frac{u_{ca}(t)}{U_{cmax}} = a\,\sin\omega t \qquad (2d)$$

$$\frac{\bar{u}_{La}(t)}{0.5\,U_s} = a\sin\omega t - \frac{8\tau_d}{\pi}\sum_{\nu}\frac{1}{\nu}\sin[\nu(\omega t+\beta-\varphi)] \qquad (2e)$$

$$\frac{u_{La1}(t)}{0.5\,U_s} = a\left(1-\frac{8\tau_d}{a\,\pi}\right)\sin(\omega t+\beta) \quad \text{for } \varphi=0 \qquad (3b)$$

$$\text{with}\quad \beta = \arcsin\left(\frac{8\tau_d}{a\,\pi}\sin\varphi\right) \qquad (3c)$$

Harmonics

The harmonics here concerned come exclusively through the switching dead time $\tau_d$ and are based on the load voltage change (Eq. 2e). Eq. 6a,b for n = 1,2,3,... resume the load voltage harmonics $u_{Lah}(t)$ and the dependences of the harmonic amplitudes $\hat{u}_{La\nu}$.

The resulting current harmonics (Eq. 7a,b) can be calculated by considering only the electromagnetic part of the machine assuming the following aproximations:

1) The inertia of the machine is so high that the motor speed does not react on the torque ripple coming through the current harmonics.
2) The smoothing effect of an eventual existing superior current control loop on the harmonics is neglected.
3) The resistive part of the machine can be neglegted compared with the reactive part for the considered harmonics. The single phase equivalent circuit of the machines are approximated by a single inductance L.

In the synchronous machine with salient type rotor the voltage harmonics see the direct axis reactance and the quadrature axis reactance alternating with the harmonic frequency $\nu\omega$. An analytical calculation of the current harmonics would need to assume a timevariant machine inductance L.

$$\frac{u_{Lah}(t)}{0.5\,U_s} = -\frac{8\tau_d}{\pi}\sum_{\nu=6n\pm1}\frac{1}{\nu}\sin[\nu(\omega t+\beta-\varphi)] \qquad (6a)$$

$$\hat{u}_{La\nu} \approx \frac{\tau_d}{\nu} \qquad \nu=6n\pm1 \qquad (6b)$$

$$\frac{i_{ah}(t)}{0.5\,U_s} = \frac{8\tau_d}{\pi}\,\frac{1}{\omega L}\sum_{\nu=6n\pm1}\frac{1}{\nu^2}\cos[\nu(\omega t+\beta-\varphi)] \qquad (7a)$$

$$\hat{i}_{a\nu} \approx \frac{\tau_d}{\omega\nu^2} \qquad \nu=6n\pm1 \qquad (7b)$$

Torque ripple

Synchronous machine. The torque ripple here considered comes only through the harmonics of the stator currents (Eq. 7a,b) together with the fundamental of the field excitation at constant load angle $\delta$ (Eq. 8a). Based on the airgap power (Eq. 8b) the torque ripple $m_h$ is calculated by Eq. 8c. Eq. 8d resumes the dependences of the harmonic amplitudes $\hat{m}_\nu$.

The current harmonics with the orders $\nu=6n-1$ build a field wave with the opposite phase sequence as the excitation field and so make a torque ripple with the orders n=6n. On the other hand the current harmonics with the orders $\nu=6n+1$ build a field wave with the same phase sequence as the excitation field and so make a torque ripple also with the orders $\nu=6n$. Adding the torque ripples with identical orders the phase shift between them causes the dependence on the angles $\varphi$ and $\delta$, so that the resulting amplitude of the torque ripple is not simply the sum of the two amplitudes.

$$e_a(t) = K_n\,n\,\sin(\omega t+\beta-\delta) \qquad (8a)$$

$$m_h\,n = e_a i_{ah} + e_b i_{bh} + e_c i_{ch} \qquad (8b)$$

$$\frac{m_h(t)}{0.5U_s} = \frac{8\tau_d}{\pi}\,\frac{3K_n}{2\omega L}\cdot \qquad (8c)$$

$$\cdot\sum_{\nu=6n}\frac{1}{\nu^2-1}\sqrt{\left(\frac{\nu+1}{\nu-1}\right)^2+\left(\frac{\nu-1}{\nu+1}\right)^2-\cos[2(\varphi-\delta)]}\cos[\nu(\omega t+\gamma_\nu)]$$

$$\hat{m}_\nu \approx \frac{\tau_d}{\omega}\,\frac{1}{\nu^2-1}\,f(\nu,\varphi,\delta) \qquad \nu=6n \qquad (8d)$$

Asynchronous machine. The torque ripple here considered comes again only through the harmonics of the stator currents (Eq. 7a,b) together with the fundamental of the stator flux. Based on the complex space vectors (park vectors) of the stator flux $\underline{\psi}_{s1}(t)$ and of the load current harmonics $\underline{i}_{Lh}(t)$ the torque ripple is calculated with Eq. 9a (p: number of pole pairs). The space vectors of the machine variables (e.g. $\underline{x}$) are generally underlined and defined by Eq. 9b. The stator flux $\underline{\psi}_{s1}(t)$ can be approximately calculated as the integral of the fundamental load voltage $u_{L1}(t)$ by neglecting stator resistance and stray flux. $a^*$ is the resulting amplitude of the load voltage according to Eq. 3a,b,c. The torque ripple $m_h(t)$ is calculated by Eq. 9c. Eq. 9d resumes the dependences of the harmonic amolitudes $\hat{m}_\nu$. $a^*$ should be kept nearly equal to the required modulation ratio by superior con-

trol and so varies nearly linear with ω.

$$m_h(t) = 3/2\ p\ \underline{x}_{s1}(t) \times i_{Lh}(t) \qquad (9a)$$

$$\underline{x}_L = 2/3\ [x_a + x_b e^{j120°} + x_c e^{-j120°}] \qquad (9b)$$

$$\frac{m_h(t)}{0.5U_s} = \frac{8 r_d}{\pi}\ \frac{3p}{2\omega L}\ \frac{a^* 0.5U_s}{\omega} \cdot \qquad (9c)$$

$$\cdot \sum_{\nu=6n} \frac{1}{\nu^2-1} \sqrt{\left(\frac{\nu+1}{\nu-1}\right)^2 + \left(\frac{\nu-1}{\nu+1}\right)^2 + \cos 2\varphi}\ \cos[\nu(\omega t + \gamma_\nu)]$$

$$\hat{m}_\nu \sim \frac{r_d}{\omega}\ \frac{a^*}{\omega}\ \frac{1}{\nu^2-1}\ f(\nu,\varphi) \qquad \nu=6n \qquad (9d)$$

The analysis in this chapter can give only a large approximation of the effects coming from the switching dead times in VSI inverter drives, for some strong simplifications are asumed (mentioned). Using the results the main limitations are:
1) Operating with very small inertias the torque ripple causes a not neglectible rotor speed ripple that again reacts back to the currents and the torque ripple. These effects can be seen in the simulation results.
2) Operating at very low modulation ratios a respectively fundamental frequencies ω there are two limiting effects: a) The neglected resistive character of the machines appears more and more. b) The load currents get discontinuous at each of their zero crossings at high switching dead times $r_d$.

## SIMULATIONS INCLUDING DISCONTINUOUS CURRENTS

Due to $r_d$ the load currents can get discontinuous at each of their zero crossings [7]. Including this operation mode an analytically description would be not practicable. The effects are investigated by computer simulation in two steps:

1) Simulation of the average values with the model of Fig.10 according to Eq. 2c and Fig. 2 with the dynamic model of the synchronous and asynchronous motor. The average load voltage during discontinuous load current is approximated linear within the discontinuous current mode. The maximum average discontinuous current $I_{dm}$ depends on the current ripple and can be roughly approximated by Eq. 10.

2) Simulation of the instantaneous values with the model of Fig. 11 with the dynamic model of the synchronous and asynchronous motor. During the switching dead time the inverter output voltage $u_a$ is dependent on the load current $i_a$ in the following way: At nonzero current, $u_a$ is equal to either the source voltage $U_s$ or zero. At zero current, $u_a$ is equal to the transformed load counter voltage ("back EMF"), which depends on the operation point (mainly on the rotor speed). Resulting in a relatively simple model the mentioned requirements can all be satisfied by the characteristic in the feedback loop of Fig. 11. If the gradient R of the characteristic at zero current is choosen according to the simulation step time $T_s$ and the approximated motor inductance L with Eq. 11, the current $i_a$ getting zero during a switching dead time makes the desired voltage $u_a$ within one simulation step. This voltage causes the current $i_a$ staying zero until the end of the switching dead time.
In order to eliminate the pulse frequency the fundamental amplitudes can be get by a simulated correlation with the fundamental frequency, while the average values are simulated with an integrator being reset at each pulse period.

A comparison of the results of the two simulation models shows no difference in simulation performance. The first model is much more practicable taking fewer simulation time (about factor 100). The simulation of Fig. 12 shows the mentioned effects with an asynchronous motor drive (changed fundamental amplitudes of voltage and current, changed average torque, voltage and current harmonics, torque ripple, effects increase with decreasing modulation ratio).

$$I_{dm} \approx 0.02 \ldots 0.04\ U_s T/L \qquad (10)$$

$$R = 1.5\ L/T \qquad (11)$$

Fundamentals
The simulated values for the fundamentals of load voltage and current as well as the average torque are plotted for nominal fundamental frequency over the slip and for nominal slip over the fundamental frequency (Fig. 13). The modulation ratio a is calculated with ω for constant magnetic flux amplitude).

Harmonics
Looking at the zero crossings of load current $i_a$ in Fig. 12 at a=0.2, The current becomes discontinuous and its average value stays near zero. During this time the average load voltage $u_{La}$ is nearly equal to the back EMF of this phase, the average behaviour of the machine is approximately identical as if this phase terminal is separated from the inverter. During one load current is discontinuous the machine begins a transient reaction towards a single phase operation point. Long before reaching stationary operation the current becomes continuous and the motor again starts a transient response towards a three phase operation point. This nonlinear limit cycle with the 6th fundamental frequency is added to the described torque ripple occurring even at exclusively continuous load currents.

## CORRECTION CIRCUITS AND MEASUREMENT RESULTS

Correction near the power electronics
These correction circuits work with each single bridge leg and are positioned near the power switches:
Murai, Watanabe and Iwasaki (1985, [3]) presented the following correction circuit. The demanded and the real voltage pulse duration get compared by an up/down counter to correct the difference within the following pulse.
Barret (1987, [8]) presented a method for minimizing the switching dead time by recognizing the OFF state of the turning OFF power switch by measuring the basis emitter voltage and then immeditely turning ON the other power switch.

Correction near the control circuits
These correction circuits influence the reference signals $u_{ca,b,c}$ invers to the effect of the switching dead time described by Eq. 2a and are positioned near the control circuits.
Kiel, Schumacher and Gabriel (1987, [9]) integrated a correction citcuit in a PWM gate array. The polarities of the motor currents are measured by an external comparator to correct the pulsewidth.
This method can be optimated for a better performance at discontinuous motor currents by using a comparator with nearly zero hysteresis and a slightly differentiating feedback. The measurement results of Fig. 14 are made with this method.
Another possibility for better performance at discontinuous motor currents is proposed in [7] (1987). At average currents below $I_{dm}$ (Eq. 10, discontinuous currents) the polarity of the current reference inputs of the current control loop are used to correct $u_{ca,b,c}$.
Viola and Grotstollen (1988, [12]) proposed a

## CONCLUSIONS

The demand for high dynamic performance of a PWM controlled AC motor drive leads to the choise of a high DC link voltage and a low motor inductance. In order to limit the current ripple the pulse frequency must be increased. With fixed power switching elements the relative switching dead time $\tau_d$ increases and causes the described effects. The motor voltage fundamental refferred to the modulation ratio gets changed and becomes depending on the operation point. The harmonics cause torque ripples with the orders $\nu=6n$ (n=1,2,..). Oszillating limit cycles occur at discontinuous motor currents. Instable subharmonic oszillations appear at some operation points. All these effects can be nearly cancelled by using a qualified correction circuit.

## REFERENCES


[1] Ueda, R.; Sonoda, T.; Inoue, Y.; Umezu, T. (1982). Unstable Oszillating Mode in PWM Variable Speed Drive of Induction Motor and its Stabilization. IEEE Ind. App. Soc. Ann. Meeting, pp. 686-691.

[2] Murai, Y.; Hosono, I.; Tunehiro, Y. (1985). On System Stability of PWM Inverter Fed Induction Motor. IEEJ Trans. Vol. 105-B, No. 5, May 1985, pp. 467-474.

[3] Murai, Y; Watanabe, T; Iwasaki, H. (1985). Waveform Distortion and Correction Circuit for PWM Inverters with Switching Lag-Times. IEEE Ind. App. Soc. Ann. Meeting, 1985, pp. 436-441.

[4] Ueda, R; Sonoda, T.; Takata, S. (1986). Experimental Results and Their Simplified Analysis on Instability Problems in PWM Inverter Induction Motor Drives. IEEE Ind. App. Soc. Ann. Meeting, 1986, pp. 196-202.

[5] Lockwood, M. (1986). Simulation of Unstable Oscillations in PWM Variable-Speed Drives. IEEE Ind. App. Soc. Ann. Meeting, 1986, pp. 575-579.

[6] Grotstollen, H.; Wang, Y.F. (1988). The Behaviour of AC Servomotors Fed by PWM Inverters with Non Negligible Switching Times. ICEM, 1988, pp. 367-372.

[7] Klug, R.D. (1987). Nonlinear Control Characteristic of PWM Four-Quadrant Choppers in Current Control Loops. EPE 1987, pp. 485-490.

[8] Barret, J. (1987). Interactive Switching in a Bridge leg. EPE 1987, pp. 185-190.

[9] Kiel, E.; Schumacher, W.; Gabriel, R. (1987). PWM Gate Array for AC Drives. EPE 1987, pp. 653-658.

[10] Heumann, K.; Schröder, H. (1988). Design Criteria for Fast Switching PWM Inverters. IEEE PESC 1988, pp. 271-276.

[11] Augsburger, F. (1988). Untersuchung der Spannungsbildung bei Pulswechselrichtern. Diplomarbeit, Inst. f. Electrical Drives, Univ. Erlangen, F.R.G.

[12] Viola, R.; Grotstollen, H. (1988). Einfluß der Ventilschaltzeiten auf das Verhalten von Pulswechselrichtern. etz-Archiv 1988, Nr. 6, pp. 181-187.

[13] Strauß, M. (1989). Untersuchung von Pulssteuerverfahren an Drehstrom-Servoantrieben. Diplomarbeit, Inst. f. Electrical Drives, Univ. Erlangen, F.R.G.


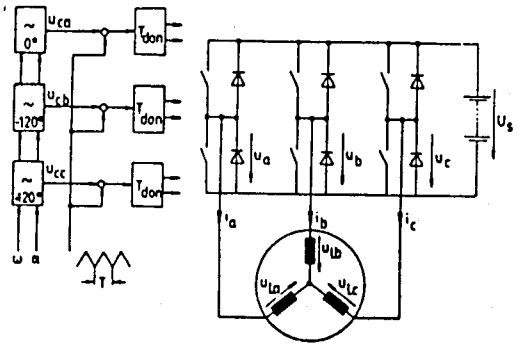


Fig. 1: PWM controlled inverter with switching dead times $T_d$

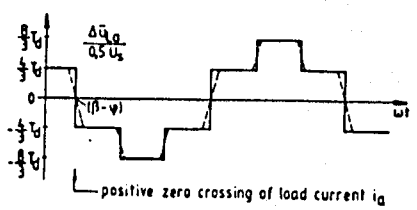


Fig. 2: Average load voltage change $\Delta\bar{u}_{La}$
—— for continuous load currents
---- including discontinuous load currents

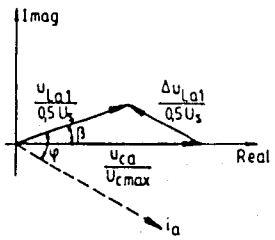


Fig. 3: Voltage fundamentals in complex time diagram

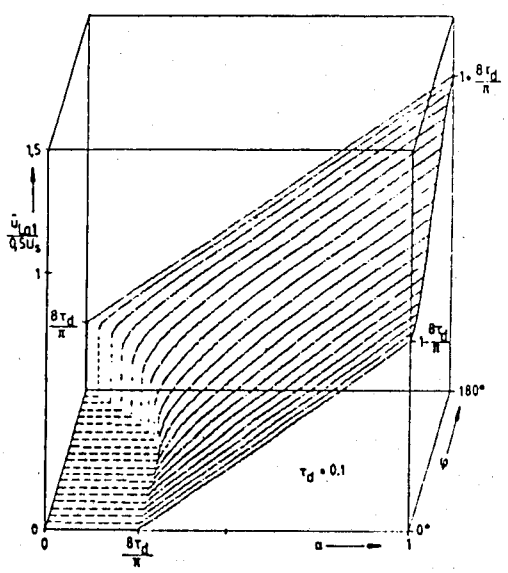


Fig. 4: Fundamental amplitude of the load voltage $\hat{u}_{La1}/0.5U_s$ depending on a and φ